Contribution from the "Grup de Quimica Quântica de l'Institut d'Estudis Catalans", Departament de Quimica, Universitat Autônoma de Barcelona, 08193 Bellaterra, Catalonia, Spain

# Anion Binding and Pentacoordination in Zinc(II) Complexes

Miquel Solà, Agusti Lledós, Miquel Duran, and Juan Bertrán*

*Received July 10, 1990*

Several tetracoordinate and pentacoordinate complexes formed by Zn(II) and the ligands water, hydroxide ion, methanol, methoxide ion, and ammonia were studied by ab initio self-consistent-field molecular orbital (SCF-MO) calculations. Complexes were chosen for their relevance to Zn-metalloenzyme chemistry. Experimental results for a trigonal-bipyramidal Zn(II) complex synthesized recently by Kimura et al. are interpreted from our calculations. It is also found that binding of an anion produces an important increase in the deprotonation energies of the ligands in the complex. Finally, inclusion of solvent effects through the cavity model gives results closer to experiment than those found for the gas phase.

## Introduction

The unusual variability and coordination flexibility of Zn(II) is well established[1] and could be an important determinant in the specificity of this cation in a number of zinc metalloenzymes.[2] Although tetrahedral geometry is usual for zinc complexes, a coordination number of 5 as a trigonal-bipyramidal (tbp) or square-pyramidal (sp) arrangement is also common.[1e,2b,3-5] Although the sp structure is catalytically unimportant, tbp pentacoordinate complexes are deemed to be essential for the catalytic action of zinc metalloenzymes. It has been suggested that, in carbonic anhydrase (CA),[6] carboxypeptidase (CPA),[7] thermolysin (TL),[8] and alcohol dehydrogenase (ADH),[9] the formation of a pentacoordinate zinc intermediate might take place. For the specific case of CA, which catalyzes the reversible hydration of $CO_2$ to yield bicarbonate anion with an extreme efficiency, it has been pointed out that the key feature in this reaction is a cyclic transition state involving five-coordinate zinc.[10] Also, the ligand exchange between bicarbonate and water may involve a pentacoordinate metal transient intermediate.[2d,6a,b] Further, inhibition of CA activity by anions such as $NCS^-$, $Au(CN)_2^-$, $HSO_3^-$, $I^-$, acetate, oxalate, and others seems to occur through binding of an anion to the fifth coordination site of zinc. This has been demonstrated experimentally by different authors,[2d,11] who have indicated that in most cases the inhibition is due to an increase in the $pk_a$ of $EZn^{II}(H_2O)$, which reduces the concentration of the catalytically active species $EZn^{II}(OH^-)$.

This was recently confirmed in a model compound as well. The zinc complex A having as ligands a phenolate-pendant macrocyclic triamine and an additional apical water in a tbp coordination was

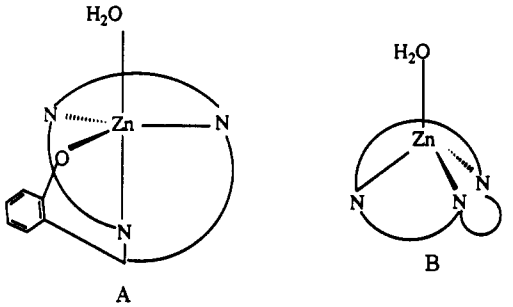


synthesized and its X-ray crystal structure reported.[4] The $pk_a$ assigned to the zinc-bound water in aqueous solution for the initial tetrahedral complex B is 7.5, but in the final five-coordinate complex A, the $pk_a$ increases to 10.7.

In spite of their importance, the study of pentacoordinate zinc complexes is relatively recent. The first X-ray crystal structure of Zn(II) with tbp coordination was reported in 1976.[12] A number of experimental works dealing with zinc pentacoordination have been published since then.[1c,d,2b,3,4,13] However, only four papers describing theoretical studies on pentacoordinate zinc complexes have appeared: the first paper studied the $Zn^{II}(H_2O)_5$ system using the semiempirical MNDO method;[14] the second paper described an ab initio study on the binding of sulfonamide and acetamide to the active site of CA by substitution of $Zn^{2+}$ by $Be^{2+}$ in model compounds;[15] the third paper carried out electrostatic and diffusional dynamics simulations in the CA active-site channel through Brownian dynamics;[16] the fourth paper performed cal-

(1) (a) Williams, R. J. P. *Polyhedron* **1987**, *6*, 61. (b) Dakternieks, D. *Coord. Chem. Rev.* **1987**, *78*, 125. (c) Kato, M.; Ito, T. *Inorg. Chem.* **1985**, *24*, 504. (d) Kato, M.; Ito, T. *Inorg. Chem.* **1985**, *24*, 509. (e) Dakternieks, D. *Coord. Chem. Rev.* **1985**, *62*, 1.
(2) (a) Lebioda, L.; Stec, B. *J. Am. Chem. Soc.* **1989**, *111*, 8511. (b) Kirchner, C.; Krebs, B. *Inorg. Chem.* **1987**, *26*, 3569. (c) Berg, J. M.; Merkle, D. L. *J. Am. Chem. Soc.* **1989**, *111*, 3759. (d) Pocker, Y.; Deits, T. L. *J. Am. Chem. Soc.* **1982**, *104*, 2424.
(3) Harrison, P. G.; Begley, M. J.; Kikabhai, T.; Killer, F. *J. Chem. Soc., Dalton Trans.* **1986**, 929.
(4) Kimura, E.; Koike, T.; Toriumi, K. *Inorg. Chem.* **1988**, *27*, 3687.
(5) McMahon, T. B.; Heinis, T.; Nicol, G.; Hovey, J. K.; Kebarle, P. *J. Am. Chem. Soc.* **1988**, *110*, 7591.
(6) (a) Haffner, P. H.; Coleman, J. E. *J. Biol. Chem.* **1975**, *250*, 996. (b) Bertini, I.; Luchinat, C. *Acc. Chem. Res.* **1983**, *16*, 272. (c) Silverman, D. N.; Lindskog, S. *Acc. Chem. Res.* **1988**, *21*, 30.
(7) (a) Kuo, L. C.; Makinen, M. W. *J. Biol. Chem.* **1982**, *257*, 24. (b) Christianson, D. W.; Lipscomb, W. N. *J. Am. Chem. Soc.* **1986**, *108*, 545. (c) Christianson, D. W.; Lipscomb, W. N. *J. Am. Chem. Soc.* **1986**, *108*, 4998. (d) Bertini, I.; Luchinat, C.; Messori, L.; Monnani, R.; Auld, D. S.; Riordan, J. F. *Biochemistry* **1988**, *27*, 8318.
(8) (a) Holmes, M. A.; Matthews, B. W. *Biochemistry* **1981**, *20*, 6912. (b) Monzingo, A. F.; Matthews, B. W. *Biochemistry* **1984**, *23*, 5724.
(9) (a) Dworschack, R. T.; Plapp, B. V. *Biochemistry* **1977**, *16*, 111. (b) Corwin, D. T., Jr.; Fikar, R.; Koch, S. A. *Inorg. Chem.* **1987**, *26*, 3079. (c) Makinen, M. W.; Yim, M. B. *Proc. Natl. Acad. Sci. U.S.A.* **1981**, *78*, 6221. (d) Makinen, M. W.; Maret, W.; Yim, M. B. *Proc. Natl. Acad. Sci. U.S.A.* **1983**, *80*, 2584. (e) Yim, M. B.; Wells, G. B.; Kuo, L. C.; Makinen, M. W. In *Frontiers in Bioinorganic Chemistry*; Xavier, A. V., Ed.; VCH: Weinheim, FRG, 1986; p 562.
(10) (a) Cook, C. M.; Haydock, K.; Lee, R. H.; Allen, L. C. *J. Phys. Chem.* **1984**, *88*, 4875. (b) Cook, C. M.; Allen, L. C. *Ann. N.Y. Acad. Sci.* **1984**, *429*, 84. (c) Cook, C. M.; Lee, R. H.; Allen, L. C. *Int. J. Quantum Chem. Symp.* **1983**, *10*, 263. (d) Allen, L. C. In *Catalytic Activation of Carbon Dioxide*; ACS Symposium Series; American Chemical Society: Washington, DC, 1988; Chapter 7, p 363.
(11) (a) Brown, R. S.; Salmon, D.; Curtis, N. J.; Kusuma, S. *J. Am. Chem. Soc.* **1982**, *104*, 3188. (b) Menziani, M. C.; Reynolds, C. A.; Richards, W. G. *J. Chem. Soc., Chem. Commun.* **1989**, 853. (c) Bertini, I.; Dei, A.; Luchinat, C.; Monnanni, R. In *Zinc Enzymes*; Bertini, I., Luchinat, C., Maret, W., Zeppezauer, M., Eds.; Birkhäuser: Boston, MA, 1986; Vol. I, p 371. (d) Eriksson, E. A.; Jones, T. A.; Liljas, A. In *Zinc Enzymes*; Bertini, I., Luchinat, C., Maret, W., Zeppezauer, M., Eds.; Birkhäuser: Boston, MA, 1986; Vol. I, p 317. (e) Mukherjee, J.; Rogers, J. I.; Khalifah, R. G. *J. Am. Chem. Soc.* **1987**, *109*, 7232. (f) Pocker, Y.; Deits, T. L. *J. Am. Chem. Soc.* **1981**, *103*, 3949.
(12) Nakacho, Y.; Misawa, T.; Fujiwara, T.; Wakawars, A.; Tomita, K. *Bull. Chem. Soc. Jpn.* **1976**, *49*, 595.
(13) (a) Bencini, A.; Bianchi, A.; Garcia-España, E.; Mangani, S.; Micheloni, M.; Orioli, P.; Paoletti, P. *Inorg. Chem.* **1988**, *27*, 1104. (b) Kai, Y.; Morita, M.; Yasuoka, N.; Kasai, N. *Bull. Chem. Soc. Jpn.* **1985**, *58*, 1631. (c) Takahashi, K.; Nishida, Y.; Kida, S. *Bull. Chem. Soc. Jpn.* **1984**, *57*, 2628. (d) Grewe, H.; Udupa, M. R.; Krebs, B. *Inorg. Chim. Acta* **1982**, *63*, 119. (e) Korp, J. D.; Bernal, I.; Merrill, C. L.; Wilson, L. J. *J. Chem. Soc., Dalton Trans.* **1981**, 1951.
(14) Giessner-Prettre, C.; Jacob, O. *J. Comput.-Aided Mol. Design* **1989**, *3*, 23.
(15) Liang, J.-Y.; Lipscomb, W. N. *Biochemistry* **1989**, *28*, 9724.

0020-1669/91/1330-2523$02.50/0 

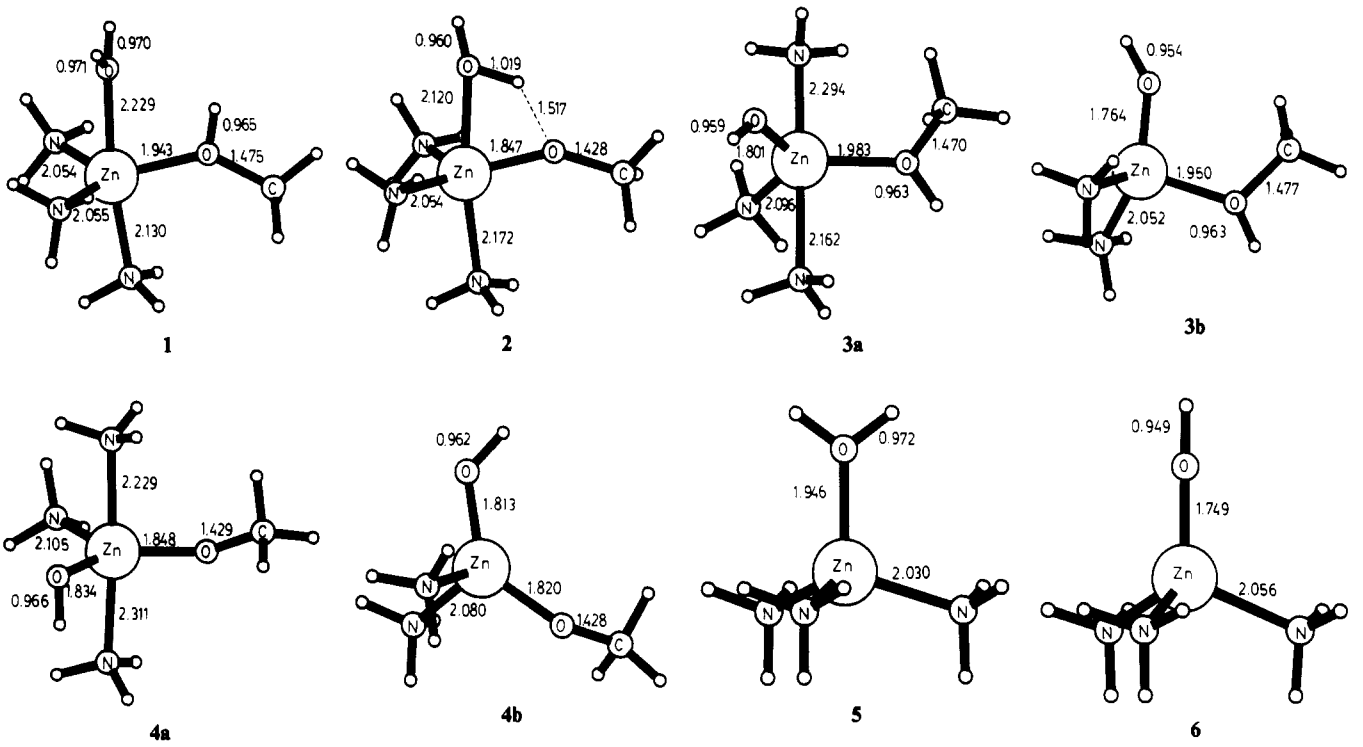


**Figure 1.** Optimized geometries of complexes **1–6**. Distances are given in Å.

culations on the $pk_a$ values of some relevant tetrahedral, sp, and octahedral complexes.[17] To date, no one has studied the structural, electronic, or energetic changes occurring in zinc complexes when their structures pass from tetrahedral to tbp geometry. Thus, to understand further the nature of these changes and how they affect the acidity of the ligands, an ab initio study of tetracoordinate and tbp pentacoordinate zinc complexes derived from model complex A has been carried out. The phenol-pendant macrocyclic triamine ligand in complex A has been modeled by one methanol and three ammonia ligands. The following sequence of complexes has been studied: $(NH_3)_3Zn^{II}(H_2O)(CH_3OH)$ (**1**), $(NH_3)_3Zn^{II}(H_2O)(CH_3O^-)$ (**2**), $(NH_3)_3Zn^{II}(OH^-)(CH_3OH)$ (**3a**), $(NH_3)_2Zn^{II}(OH^-)(CH_3OH)$ (**3b**), $(NH_3)_3Zn^{II}(OH^-)(CH_3O^-)$ (**4a**), $(NH_3)_2Zn^{II}(OH^-)(CH_3O^-)$ (**4b**), $(NH_3)_3Zn^{II}(H_2O)$ (**5**), and $(NH_3)_3Zn^{II}(OH^-)$ (**6**).

Since the experimental $pk_a$ values were obtained in aqueous solution, the effect of water has been included in our calculations through a continuum model, so a more realistic description of the properties of these complexes can be obtained.

## Methods

Ab initio all-electron RHF–SCF calculations were performed for complexes **1–6**. The large size of the systems prevents use of extended basis sets with polarization and diffuse functions. However, since the purpose of this paper is merely to compare a series of analogous systems, a semiquantitative level of calculation through use of a split-valence double-$\zeta$ basis set is sufficient. The 3-21G basis set[18] was used for all atoms except for the hydrogens of the $NH_3$ and $CH_3$ groups, for which the STO-3G[19] basis set was used. Geometry optimizations were carried out by means of the Broyden–Fletcher–Goldfarb–Shanno[20] algorithm using gradients calculated analytically. Geometries of the $NH_3$ and $CH_3$ groups were kept frozen at the fully optimized geometry of the $NH_3$ and $CH_3OH$ molecules by using the aforementioned mixed basis set.[21]

**Table I.** Experimental Geometric Parameters of Complex A and Calculated Geometrical Parameters of Complex **2** (Distances in Å and Angles in deg)

| param | exptl | calc | param | exptl | calc |
|---|---|---|---|---|---|
| $d_{Zn-O_w}$ | 2.219 | 2.120 | $\angle N_aZnO_m$ | 91.4 | 98.8 |
| $d_{Zn-N_a}$ | 2.139 | 2.172 | $\angle N_aZnN_{eq2}$ | 87.4 | 94.4 |
| $d_{Zn-O_m}$ | 1.930 | 1.847 | $\angle N_aZnO_w$ | 174.4 | 170.5 |
| $d_{Zn-N_{eq1}}$ | 2.029 | 2.052 | $\angle N_{eq1}ZnN_{eq2}$ | 108.3 | 117.2 |
| $d_{Zn-N_{eq2}}$ | 2.050 | 2.052 | $\angle N_{eq1}ZnO_m$ | 113.0 | 118.8 |
| $\angle N_aZnN_{eq1}$ | 90.3 | 96.0 | $\angle N_{eq2}ZnO_m$ | 138.7 | 120.4 |

Nonetheless, their relative positions in the coordination sphere of the zinc atom were optimized. To introduce the solvent effect, the SCRF model due to Tomasi et al.[22] was used. In this model, the solvent is represented by a continuous polarizable dielectric with permitivity $\epsilon$ (e.g., $\epsilon$ = 78.36 for water), and the solute is placed inside a cavity accurately defined by its own geometry. Dielectric polarization due to the solute is simulated by the creation of a system of virtual charges on the cavity surface. The charge distribution on the surface polarizes in turn the charge distribution in the solute. This process is iterated until obtaining self-consistency in the solute electron density. The electrostatic contribution to the solvation free energy is found as the difference between the free energies computed with the continuum model and without it. Moreover, the cavitation free energy is calculated with Pierotti's equation.[23] The optimized geometries in the gas phase were used throughout. All calculations were performed through use of the MONSTERGAUSS program.[24,25] The solvent effect was studied with a version of this written program by Tomasi and co-workers to account for the reaction field created by the solvent.

## Results and Discussion

**1. Gas-Phase Results. Geometries.** Figure 1 shows the most important geometric parameters obtained in the optimization of complexes **1–6**. In complex **1**, water and methanol are axial and

(16) Reynolds, J. C. L.; Cooke, K. F.; Northrup, S. H. *J. Phys. Chem.* **1990**, *94*, 985.
(17) Bertini, I.; Luchinat, C.; Rosi, M.; Sgamellotti, A.; Tarantelli, F. *Inorg. Chem.* **1990**, *29*, 1460.
(18) (a) Binkley, J. S.; Pople, J. A.; Hehre, W. J. *J. Am. Chem. Soc.* **1980**, *102*, 939. (b) Dobbs, K. D.; Hehre, W. J. *J. Comput. Chem.* **1987**, *8*, 861.
(19) Hehre, W. J.; Stewart, R. F.; Pople, J. A. *J. Chem. Phys.* **1969**, *51*, 2657.
(20) (a) Broyden, C. G. *Math. Comp.* **1970**, *24*, 365. (b) Fletcher, R. *Comput. J.* **1970**, *13*, 317. (c) Goldfarb, D. *Math. Comp.* **1970**, *24*, 23. (d) Shanno, D. F. *Math. Comp.* **1970**, *24*, 647.
(21) The values used for the $NH_3$ and $CH_3$ are the following: $d_{N-H}$ = 1.026 Å, $\angle HNH$ = 109.5°; $d_{C-H}$ = 1.098 Å, $\angle HCH$ = 109.7°.
(22) (a) Miertuš, S.; Scrocco, E.; Tomasi, J. *Chem. Phys.* **1981**, *55*, 117. (b) Pascual-Ahuir, J. L.; Silla, E.; Tomasi, J.; Bonaccorsi, R. *J. Comput. Chem.* **1987**, *8*, 778. (c) Floris, F.; Tomasi, J. *J. Comput. Chem.* **1989**, *10*, 616.
(23) Pierotti, R. A. *Chem. Rev.* **1976**, *76*, 717.
(24) Peterson, M. R.; Poirier, R. A. Program MONSTERGAUSS. Department of Chemistry, University of Toronto, Toronto, Ontario, Canada, 1986.
(25) The sphere radii used for atoms were 20% larger than the van der Waals (or ionic) radii (hydrogen, 1.44 Å; carbon, 1.94 Å; nitrogen, 1.80 Å; oxygen, 1.68 Å; zinc, 0.84 Å). The solvent effect calculations were carried out at 298.15 K.

equatorial ligands, respectively, giving rise to an almost regular tbp arrangement. This is confirmed by the value of the axial angle $\angle N_{ax}ZnO_w$, which is almost linear (171.9°), and by the sum of the equatorial angles (118.8° for $\angle N_{eq1}ZnN_{eq2}$, 120.8° for $\angle N_{eq2}ZnO_m$, and 118.8° for $\angle O_mZnN_{eq1}$), which is almost 360.0° (358.4°). As already predicted theoretically by Rossi and Hoffmann[26] and confirmed later by experimental work in Zn(II) complexes,[1c,d,3,4,13] axial bonds lengths are longer than equatorial bond lengths in $d^{10}$ tbp complexes like complex **1**.

In Table I we collect the most important geometric parameters of the experimental complex A, synthesized by Kimura et al.,[4] and of geometry-optimized complex **2**, which is used in this work to model complex A. The difference between the experimental and theoretical values is very small and never larger than 5%. The angles do not agree so well, although the disagreement is due, to some extent, to the different nature of the ligands containing N atoms. Whereas the experimental complex has a phenol-pendant macrocyclic triamine with the three nitrogens connected by methylene groups forming a molecular ring, the theoretical model **2**, used to represent complex A, contains three ammonia groups having fewer geometry constraints. The optimized structure of complex **2** is a slightly distorted tbp with water in an axial site and a $CH_3O^-$ anion as an equatorial ligand. This structure agrees with the hypothesis stated by Rossi and Hoffmann[26] that the stronger $\sigma$ donor prefers the equatorial sites of a tbp for $d^{10}$ $ML_5$ complexes. As in complex **1**, the axial bonds are longer than the equatorial ones. Interestingly, there is an intramolecular hydrogen bond between the oxygen of the $CH_3O^-$ group and one of the hydrogens of water, which accounts, in part, for the distortion of the tbp geometry.

If the optimization is started from complex $(NH_3)_3Zn^{II}(OH^-)_{eq}(CH_3OH)_{eq}$ with hydroxide and methanol as equatorial ligands, complex **3a** (see Figure 1) is obtained. This complex has an almost regular tbp arrangement, with an axial angle $\angle N_{ax1}ZnN_{ax2}$ of 173.5° and equatorial angles of 125.1° ($\angle O_wZnN_{eq}$), 116.6° ($\angle N_{eq}ZnO_m$), and 118.3° ($\angle O_mZnO_w$) adding up exactly to 360.0°. Conversely, if the optimization is started from complex $(NH_3)_3Zn^{II}(OH^-)_{ax}(CH_3OH)_{eq}$ with an axial hydroxide and an equatorial methanol, a free ammonia molecule is formed and the distorted tetrahedral complex **3b** is found. Therefore, this pentacoordinate complex, with an axial hydroxide, is not a minimum in the full potential energy hypersurface. As shown by Rossi and Hoffmann,[26] $\sigma$ donors stabilize a tbp when located in equatorial sites. In contrast, this geometry is unfavored when $\sigma$ donors are placed in axial sites. Therefore, the presence of a hydroxide group in an axial position explains the breaking of the initial tbp geometry.

Initially, the optimization of complex **4a** was started with the hydroxide ion in an axial position of the tbp. However, since the optimization process let the variable parameters free to change, during this optimization the hydroxide moved to an equatorial site, as expected from the Rossi and Hoffmann hypothesis[26] on the preferences of $\sigma$ donors for equatorial positions in tbp complexes. The axial angle $\angle N_{ax1}ZnN_{ax2}$ is 173.6°, and the total of the equatorial angles of 113.4° ($\angle O_wZnN_{eq}$), 109.7°, ($\angle N_{eq}ZnO_m$), and 136.8° ($\angle O_mZnO_w$) is 359.9°. An interesting point concerns the Zn–N axial distances in complexes **3a** and **4a**, which differ by ca. 0.1 Å. This difference had been already observed in some experimental distorted tbp complexes.[2b,13a,c]

Calculations have shown that neither $(NH_3)_3Zn^{II}(OH^-)_{ax}(CH_3OH)_{eq}$ nor $(NH_3)_3Zn^{II}(OH^-)_{ax}(CH_3O^-)_{eq}$ is a stable compound. Any optimization process starting from these structures must lead to stable complexes (true minima in the potential energy hypersurface). If there are a number of possible minima in the hypersurface, the final result is very dependent on the geometry of the starting point and the optimization method employed. This fact justifies why complex $(NH_3)_3Zn^{II}(OH^-)_{ax}(CH_3O^-)_{eq}$ changes to complex $(NH_3)_3Zn^{II}(OH^-)_{eq}(CH_3O^-)_{eq}$, whereas $(NH_3)_3Zn^{II}(OH^-)_{ax}(CH_3OH)_{eq}$ complex decomposes to **3b** and $NH_3$.

Table II. Binding Energies (BE) in kcal/mol for the Different Ligands, Where L,$x \rightarrow y$ Means That Ligand L Joins Complex $x$ To Give $y$

| ligand | BE | ligand | BE |
|---|---|---|---|
| $CH_3OH$,**5** → **1** | −40.1 | $CH_3O^-$,**6** → **4a** | −170.0 |
| $CH_3O^-$,**5** → **2** | −290.3 | $NH_3$,**3b** → **3a** | −14.3 |
| $CH_3OH$,**6** → **3a** | −20.4 | $NH_3$,**4b** → **4a** | −4.8 |

For comparison purposes, tetracoordinate complexes **4b**, **5**, and **6** have been also optimized. In particular, complex **5** is our model for the experimental complex B. All these three systems exhibit an almost regular tetrahedral geometry. For instance, the ∠NZnO angles are 101.3, 107.7, and 113.4° for complexes **4b**, **5**, and **6**, respectively.

When one compares the Zn–N bonds for the different optimized species, one can see that the tetrahedral Zn–N bond lengths are similar to the equatorial tbp Zn–N bond lengths. The axial Zn–N bonds are 4% to 6% longer than equatorial bonds for complexes **1** and **2**, these percentages being similar to those found experimentally.[13d] Regarding the Zn–O bonds, their length depends on the number of ligands, the total charge of the complex, and the location of the ligand. Our results show that this bond lengthens when the number of ligands increases (compare **1** and **5**, **3a** and **3b**, or **4a** and **4b**) and when the total positive charge of the complex increases (compare **1** and **2** or **5** and **6**). It is also found that the Zn–O axial bonds are always longer than the Zn–O equatorial bonds.

**Energetics.** In Table II we report the most important binding energies (BE) of the different ligands obtained from the total energies of the zinc complexes studied. From this table, one can see that the binding energy of $CH_3O^-$ to complex **5** is larger than that of $CH_3OH$ to the same complex by 250.2 kcal/mol, so the $Zn–O_m$ bond in complex **2** is stronger than in complex **1**. This point is reinforced by the Mayer bond orders[27] of the two $Zn–O_m$ bonds, which are 0.584 and 0.355 for complexes **2** and **1**, respectively. Similarly, the binding of $CH_3OH$ to complex **6** yields pentacoordinate complex **3a** by release of only 20.4 kcal/mol, whereas the binding of $CH_3O^-$ to complex **6** leads to complex **4a** by release of 170.0 kcal/mol. The binding energy of $CH_3OH$ to tetracoordinate complexes **5** and **6** to yield **1** and **3a**, respectively, differs only by 19.7 kcal/mol. On the contrary, the binding energy of $CH_3O^-$ is remarkably different if one of the four ligands is water (**5**) or hydroxide (**6**). In particular, the binding energy of $CH_3O^-$ to complex **5** to yield complex **2** is −290.3 kcal/mol and decreases to −170.0 kcal/mol for complex **6** to yield **4a**. Therefore, the loss of a water proton to yield a hydroxide ligand reduces the strength of the bond between Zn and the $CH_3O^-$ ligand by 120.3 kcal/mol due to the increase of the electron density around the zinc atom. This can be related to the carbonic anhydrase mechanism in which the deprotonation of water in the active site of the enzyme should facilitate the release of an $HCO_3^-$ anion to regenerate the enzyme in its active form.[2d,6c] Another important feature is that, in obtaining complex **4a** from **4b** and a $NH_3$ molecule, one finds the release of only 4.8 kcal/mol, which gives a quantitative idea on the precarious stability of pentacoordinate zinc(II) complexes with two anions in its coordination sphere. In fact, some authors have already stated the hypothesis that the $Zn^{2+}$ ion in the active site of carbonic anhydrase apparently cannot accommodate two negative charges in its inner sphere.[11f] As mentioned before, complex **4a** is only stable when the two strong $\sigma$ donors ($CH_3O^-$ and $OH^-$) are located in equatorial sites. The pentacoordinate complex $(NH_3)_3Zn^{II}(OH^-)_{ax}(CH_3OH)_{eq}$, with an axial hydroxide ligand and a total positive charge of one, is unstable and splits into tetracoordinate complex **3b** and the ammonia molecule during the optimization process. Loss of this $NH_3$ molecule to yield **3b** is more favorable by 6.2 kcal/mol than loss of a $CH_3OH$ ligand to give complex **6**. This difference does not change in stable complex **3a** with the hydroxide in equatorial site, where the binding energy of $NH_3$ is 14.3 kcal/mol and that of $CH_3OH$ is 20.4 kcal/mol.

(26) Rossi, A. R.; Hoffmann, R. *Inorg. Chem.* **1975**, *14*, 365.

(27) Mayer, I. *Int. J. Quantum Chem.* **1986**, *29*, 477.

**Table III.** Deprotonation Energies (DPEs) in kcal/mol for the Different Species Studied, Where Relevant Ligands for the Different Complexes Appear within Parentheses

| species | DPE |
|---|---|
| $H_2O/OH^-$ | 450.1 |
| $CH_3OH/CH_3O^-$ | 430.9 |
| $Zn^{II}(H_2O)/Zn^{II}(OH^-)$ | 102.4 |
| $Zn^{II}(CH_3OH)/Zn^{II}(CH_3O^-)$ | 109.8 |
| **1**($CH_3OH$, $H_2O$)/**2**($CH_3O^-$, $H_2O$) | 180.7 |
| **1**($CH_3OH$, $H_2O$)/**3a**($CH_3OH$, $OH^-$) | 194.6 |
| **2**($CH_3O^-$, $H_2O$)/**4a**($CH_3O^-$, $OH^-$) | 295.2 |
| **3a**($CH_3OH$, $OH^-$)/**4a**($CH_3O^-$, $OH^-$) | 281.3 |
| **3b**($CH_3OH$, $OH^-$)/**4b**($CH_3O^-$, $OH^-$) | 271.9 |
| **5**($H_2O$)/**6**($OH^-$) | 174.9 |

To assess further the importance of the intramolecular hydrogen bond between the $H_2O$ and $CH_3O^-$ ligands in complex **2**, we have optimized this complex with the restriction of freezing the geometry of water and not allowing the formation of an intramolecular hydrogen bond. In this case, the total energy turns out to be 15.4 kcal/mol higher than the energy of complex **2** optimized without such restrictions. This result shows that this intramolecular hydrogen bond contributes partially to the final stability of tbp complex **2**.

Table III collects for some of the studied species the gas-phase deprotonation energies (DPEs), which are a first indication of the acidity of the coordinated species. The first interesting feature concerns the diminution in the DPEs of the water and methanol molecules by more than 300 kcal/mol due to the presence of zinc. This decrease in the DPE of water coordinated to zinc has been already pointed out by different authors.[14,28,29] Likewise, Pullmann and Demoulin,[28] and also Kitchen and Allen,[29] have already reported 158.1 and 166.8 kcal/mol, respectively, for the DPE of complex **5** using pseudopotentials for zinc. These values do not differ very much from our computed value of 174.9 kcal/mol.

Deprotonation of methanol in complex **1** is easier than deprotonation of water by 13.9 kcal/mol. The DPE of $H_2O$ coordinated to Zn(II) increases by 72.5 kcal/mol when the dication is also coordinated to three $NH_3$ molecules (compare the DPE of $Zn^{II}(H_2O)$ and complex **5**). The additional coordination of methanol to complex **5** increases slightly the DPE of water (compare the DPE of water in complexes **1** and **5**). This is due to the charge transfer from ligands, which prevents the proton release. The DPEs of $H_2O$ in complexes **1** and **5** differ only by 19.7 kcal/mol, showing that deprotonation energies are not significantly affected by the change in the number of neutral ligands. However, when the incoming fifth ligand is negatively charged, the DPE increases substantially. In particular, the DPE of water in pentacoordinate complex **2** is 120.3 kcal/mol larger than the DPE of water in tetracoordinate complex **5**. This can be compared to the change in the $pk_a$ of the water ligand in the experimental complex B (modeled here as complex **5**), which changes from 7.5 to 10.7 when an incoming phenolate ligand is coordinated to the zinc dication.[4] Similarly, the DPE of methanol in complex **3a**, which has a hydroxide ligand, is remarkably larger than that of methanol in complex **1**.

**Charges.** The Mulliken charges of the zinc atom and the coordinated ligands for the studied species are collected in Table IV. It should be noted that complexes **3a** and **4a** have one equatorial and two axial $NH_3$ ligands, so for them the equatorial and axial charges of ammonia in Table IV have been interchanged. Despite the well-known basis set dependence of Mulliken populations, they are useful to establish qualitative comparisons between similar complexes, which is the aim we pursue here.

The charge on the zinc atom does not change very much among the different species, the largest being found in complex **1** (1.382 au) and the smallest charge being found in complex **4b** (1.052 au). As expected, the most important factor accounting for the variation in the charge of the zinc atom is the overall positive charge of the complex: the larger the total positive charge is, the larger the positive charge is on the zinc atom. There is also another factor, namely the coordination number around the zinc atom. Surprisingly, as the coordination number increases, the positive charge on the zinc atom increases too (compare **1** and **5**, **2** and **6**, **3a** and **3b**, or **4a** and **4b**). The reason may be that charge transfer from ligands to zinc decreases as a result of the longer zinc–ligand bonds, which are common among pentacoordinate complexes. The hydrogen atom of water in complex **5** bears a greater positive charge than that of complex **1** (0.496 vs 0.458, respectively), so the water ligand of tetracoordinate complex **5** is easier to deprotonate than the water ligand of pentacoordinate complex **1**. Similarly, the hydroxide group becomes more nucleophilic when an $NH_3$ molecule is added to complexes **3b** or **4b** to yield **3a** or **4a**, respectively. Finally, in all complexes the $NH_3$ equatorial ligands are more positively charged than the $NH_3$ axial ligands. This fact can be explained by taking into account that the axial sites of a tbp $d^{10}$ $ML_5$ complex have an excess of electrons,[26] so the axial ammonia molecules can transfer less charge to the zinc atom than the equatorial molecules.

**2. Solvent Effects.** In order to analyze the stability and acidity of the complexes in aqueous solution, the solvent effect has been introduced through use of the cavity model of Tomasi et al.[22] using the geometry optimized in the gas phase. Table V reports the solvation free energies and their components ($\Delta G_{el}$ and $G_{cav}$) for complexes **1**–**6** in aqueous solution. One can see that the effect of the solvent is always stabilizing. The larger the total positive charge is, the more stabilized the complex becomes in solution. Moreover, the stabilization is larger for tetracoordinate complexes than for pentacoordinate complexes. Two related factors can be addressed: on one hand, tetracoordinated complexes have a smaller cavitation energy, and on the other hand, they have a larger electrostatic contribution to the free energy.

The binding free energies (BFE) of the different ligands to the zinc atom in aqueous solution are given in Table VI. Upon comparison with values of Table II, one realizes that all binding energies have diminished by the effect of the solvent. This decrease in BFE is due to a smaller charge transfer from ligands to zinc. In fact, the charges move to the outer sites of the complex to interact more strongly with the solvent represented here by a polarizable dielectric. This leads usually to a looser zinc–ligand bond. This point is stressed by the Mayer bond orders, which decrease for all Zn–O bonds yet oscillate for the Zn–N bonds. The same reason can be addressed to explain the increase in the observed positive charge for zinc. These effects cause complex **4a** to be unstable in solution. Although pentacoordinate complex **3a**, which has an equatorial hydroxide, is still stable in solution, its decomposition to methanol and complex **6** is easier (1.2 kcal/mol) than release of $NH_3$ and formation of complex **3b** (3.5 kcal/mol). Regarding atomic charges, although the Mulliken populations of the zinc d orbitals do not change at all, the populations of the 4s and 4p orbitals decrease noticeably. For instance, in complex **1** the zinc charge increases from 1.382 to 1.401 electrons whereas the 4s and 4p Mulliken populations decrease from 0.751 to 0.733 electrons from the gas phase to solution. Finally, it is worth noting that solvent effects decrease the stabilization of the intramolecular hydrogen bond of complex **2** from 15.4 kcal/mol in the gas phase to 11.3 kcal/mol in solution.

Table VII collects the proton-transfer energies (PTEs) in the gas phase and free energies in solution for reaction 1.

$$AH + H_2O \rightarrow A^- + H_3O^+ \quad (1)$$

Relative to the gas phase, in aqueous solution the differences between the PTEs of the studied species are lowered. For complexes **1** and **5** we have obtained exothermic proton transfers in the gas phase. On the contrary, in solution these proton transfers become endothermic processes. This result is closer to experiment, showing that inclusion of solvent effects is essential to get a more realistic description of the proton-transfer processes. In particular, for complex B (modeled here as **5**), which has an experimental $pk_a$ value of 7.5,[4] we have obtained −16.6 and 40.3 kcal/mol for the proton transfer in the gas phase and in solution, respectively.

(28) Pullman, A.; Demoulin, D. *Int. J. Quantum Chem.* **1979**, *16*, 641.
(29) Kitchen, D. B.; Allen, L. C. *J. Phys. Chem.* **1989**, *93*, 7265.

**Table IV.** Charges (au) on the Zinc Atom and on Coordinated Ligands for the Studied Species

| species | coord no. | tot. charge | Zn | $H_2O$ (or $OH^-$) | $CH_3OH$ (or $CH_3O^-$) | $(NH_3)_{eq1}$ | $(NH_3)_{eq2}$ | $(NH_3)_{ax}$ |
|---|---|---|---|---|---|---|---|---|
| **1** | 5 | +2 | 1.382 | 0.140 | 0.135 | 0.120 | 0.121 | 0.101 |
| **5** | 4 | +2 | 1.344 | 0.190 | | 0.156 | 0.156 | 0.156 |
| **2** | 5 | +1 | 1.299 | 0.043 | −0.600 | 0.092 | 0.092 | 0.076 |
| **6** | 4 | +1 | 1.219 | −0.539 | | 0.107 | 0.107 | 0.107 |
| **3a** | 5 | +1 | 1.245 | −0.547 | 0.105 | 0.054 (ax) | 0.064 (ax) | 0.079 (eq) |
| **3b** | 4 | +1 | 1.209 | −0.530 | 0.113 | 0.107 | 0.107 | |
| **4a** | 5 | 0 | 1.115 | −0.574 | −0.650 | 0.028 (ax) | 0.035 (ax) | 0.049 (eq) |
| **4b** | 4 | 0 | 1.052 | −0.555 | −0.628 | 0.066 | 0.066 | |

**Table V.** Values of the Electrostatic Contribution ($\Delta G_{el}$) to the Solvation Free Energy, Free Energy of Cavitation ($G_{cav}$), and Their Sum ($\Delta G_{solv}$) at 298 K for the Different Complexes Studied, Where All Energies Are Given in kcal/mol

| species | $\Delta G_{el}$ | $G_{cav}$ | $\Delta G_{solv}$ |
|---|---|---|---|
| **1** | −180.6 | 19.7 | −160.9 |
| **2** | −54.3 | 19.3 | −35.0 |
| **3a** | −55.3 | 19.0 | −36.3 |
| **3b** | −61.2 | 17.6 | −43.6 |
| **4a** | −20.5 | 18.9 | −1.6 |
| **4b** | −24.8 | 17.4 | −7.4 |
| **5** | −195.5 | 16.6 | −178.9 |
| **6** | −63.7 | 16.0 | −47.7 |

**Table VI.** Binding Free Energies (BFEs) in kcal/mol of the Different Ligands in Aqueous Solution, Where L,$x \rightarrow y$ Means That Ligand L Joins Complex $x$ To Give $y$

| ligand | BFE | ligand | BFE |
|---|---|---|---|
| $CH_3OH$,**5** → **1** | −14.3 | $CH_3O^-$,**6** → **4a** | −49.3 |
| $CH_3O^-$,**5** → **2** | −71.6 | $NH_3$,**3b** → **3a** | −3.5 |
| $CH_3OH$,**6** → **3a** | −1.2 | $NH_3$,**4b** → **4a** | 4.4 |

**Table VII.** Proton-Transfer Energies in the Gas Phase and Proton-Transfer Free Energies in Solution for Reaction 1 for the Different $AH/A^-$ Species Studied, Where Energies Are Given in kcal/mol

| species | $\Delta E_{PT,gas}$ | $\Delta G_{PT,solv}$ |
|---|---|---|
| $H_2O/OH^-$ | 258.5 | 93.7 |
| $CH_3OH/CH_3O^-$ | 239.3 | 97.8 |
| **1**($CH_3OH$, $H_2O$)/**2**($CH_3O^-$, $H_2O$) | −10.9 | 40.5 |
| **1**($CH_3OH$, $H_2O$)/**3a**($CH_3OH$, $OH^-$) | 3.0 | 53.4 |
| **2**($CH_3O^-$, $H_2O$)/**4a**($CH_3O^-$, $OH^-$) | 103.6 | 62.6 |
| **3a**($CH_3OH$, $OH^-$)/**4a**($CH_3O^-$, $OH^-$) | 89.7 | 49.7 |
| **3b**($CH_3OH$, $OH^-$)/**4b**($CH_3O^-$, $OH^-$) | 80.3 | 41.8 |
| **5**($H_2O$)/**6**($OH^-$) | −16.7 | 40.3 |

Clearly, the gas-phase result cannot account for the experimental $pk_a$ value.

For $H_2O$ and $CH_3OH$ the ordering of the proton transfer in the gas-phase energies is reversed in solution, water being more easily deprotonated than methanol. In complex **1**, deprotonation of $CH_3OH$ is easier than that found for $H_2O$, both in the gas phase and in solution, in complete agreement with the experimental results reported by Kimura et al.[4] As in the gas phase, the $\Delta G_{PT,solv}$ values of water in complexes **2** and **5**, which differ by 22.3 kcal/mol, helps to explain the different $pk_a$ values of the water ligand in the experimental species related with **2** and **5**, which are 10.7 and 7.5, respectively.[4] Therefore, these theoretical results reinforces the experimental ones, showing the important decrease on the water acidity when an incoming anion is bonded as a fifth ligand. This result is important in order to explain some mechanistic aspects of reaction and inhibition in carbonic anhydrase.

## Conclusions

Complexes **1**–**6** have been studied at an ab initio level of theory through use of the mixed basis set explained in the methods part.

As predicted by Rossi and Hoffmann,[26] $\sigma$ donors prefer the equatorial sites of a trigonal bipyramid for these $d^{10}$ $ML_5$ complexes. As expected, binding of anions to a tetracoordinate complex is more exothermic than binding of neutral ligands. Thus, pentacoordinate Zn(II) complexes are favored when the incoming fifth ligand is located at an equatorial site and is anionic. Binding of an anion brings about an important increase in the deprotonation energies of the other ligands in the complex. This can be related to anionic inhibition in carbonic anhydrase.

Inclusion of solvent effects through the cavity model reduces all binding energies. In particular, complex **4a** has been found to be unstable in aqueous solution. The deprotonation free energies found in solution are closer to experiment that those found in the gas phase. Although the level of calculation employed does not allow for an accurate evaluation of the $pk_a$, the correct ordering in the proton affinities of the different ligands in the studied complexes has been reproduced by our calculations.

**Acknowledgment.** We wish to thank Prof. Tomasi for kindly providing us with a copy of his continuum model program. We gratefully acknowledge the economic support of the Commission of the European Communities (CEE) under Contract SC1.0037.C.